

## Electronic Supplementary Information

### **Tetrasubstituted imidazole-based multifunctional fluorophores: trace water detection and lipid droplets (LDs) imaging studies**

Mohammad Masood Zafar,<sup>a</sup> Rashmi Yadav,<sup>b</sup> Alok Singh,<sup>a</sup> Nidhi Tyagi,<sup>c\*</sup> Animesh Samanta,<sup>b\*</sup> and Rakesh K. Mishra<sup>a\*</sup>

---

<sup>a</sup>Department of Chemistry, National Institute of Technology Uttarakhand (NITUK), Srinagar (Garhwal)-246174, Uttarakhand, India.

<sup>c</sup>Molecular Sensors and Therapeutics Research Laboratory, Department of Chemistry, Shiv Nadar Institution of Eminence, Delhi NCR, NH 91, Tehsil Dadri, Gautam Buddha Nagar-201314, Uttar Pradesh, India.

<sup>b</sup>School of Chemical Sciences, Amity University Punjab, Sector 82A, IT City, International Airport Road, Mohali-140306, Punjab, India.

## Table of Contents

S. No.	Experimental Details	Page No
1	General Experimental Details.....	S3
1.1	Synthesis-General Procedures.....	S3
1.2	Measurements and Methods.....	S3
1.2.1	Cell Viability Experiment.....	S3
1.2.2	Cellular Co-localization Experiment.....	S4
2	Synthesis and Characterization.....	S4-S5
3	FT-IR, <sup>1</sup> H NMR, <sup>13</sup> C NMR, and HRMS Spectra of <b>TSIm-1</b> and <b>TSIm -2</b> (Figure S1-S7).....	S5-S8
4	Theoretical Studies of <b>TSIm-1</b> & <b>TSIm-2</b> (Figure S8).....	S9
5	Photophysical properties of <b>TSIm-1</b> and <b>TSIm-2</b> in solid state.....	S10
5.1	Solid states luminescence behaviour of compound <b>TSIm-1</b> and <b>TSIm-2</b> (Figure S9).....	S10
5.2	Absorption spectra of <b>TSIm-1</b> and <b>TSIm-2</b> in different Solvents (Figure S10).....	S10
6	Demonstration of TICT Process (Figure S11).....	S11
7	Aggregation studies of compounds <b>TSIm-1</b> and <b>TSIm-2</b> (Figure S12-S14).....	S12-S14
7.1	Aggregation studies of <b>TSIm-1</b> and <b>TSIm-2</b> in THF/Water mixture (Figure S12).....	S12
7.2	Aggregation studies of <b>TSIm-1</b> and <b>TSIm-2</b> in DMSO/Water mixture (Figure S13).....	S13
7.3	Aggregation studies of <b>TSIm-1</b> and <b>TSIm-2</b> in ACN/Water mixture (Figure S14).....	S14
8	Dynamic Light Scattering (DLS) and SEM studies <b>TSIm-1</b> <sub>Agg</sub> and <b>TSIm-2</b> <sub>Agg</sub> .....	S15-S16
8.1	DLS data of <b>TSIm-1</b> in organic solvent and 90% H <sub>2</sub> O fractions (Table S2).....	S15
8.2	SEM images of <b>TSIm-1</b> <sub>Agg</sub> (Figure S15).....	S15
8.3	DLS data of <b>TSIm-2</b> in organic solvent and 90% H <sub>2</sub> O fractions (Table S3).....	S16

<b>8.4</b>	SEM images of <b>TSIm-1<sub>Agg</sub></b> (Figure S16)	<b>S16</b>
<b>9</b>	<sup>1</sup> H NMR Studies of <b>TSIm-1</b> with D <sub>2</sub> O (Figure S17)	<b>S17</b>
<b>9.1</b>	<sup>1</sup> H NMR Titration Studies of <b>TSIm-1</b> with different D <sub>2</sub> O concentration (Table S3)	<b>S17</b>
<b>10</b>	Imaging pattern obtained by <b>TSIm-1</b> triggered by different trace water input (Figure S18)	<b>S18</b>
<b>11</b>	Trace water detection property of <b>TSIm-2</b> (Figure S19)	<b>S18</b>
<b>12</b>	Photostability of <b>TSIm-1</b> and <b>TSIm-2</b> (Figure S20)	<b>S19</b>
<b>13</b>	Cytotoxicity studies of <b>TSIm-1</b> and <b>TSIm-2</b> in HeLa cell line (Figure S21)	<b>S19</b>
<b>14</b>	Cytotoxicity studies of <b>TSIm-1</b> and <b>TSIm-2</b> in HepG2 cell line (Figure S22)	<b>S19</b>
<b>15</b>	Fluorescence imaging with <b>TSIm-2</b> and response without/with oleic Acid (Figure S23)	<b>S20</b>
<b>16</b>	Monitoring of LDs generation in HepG2 cells via flow cytometry with <b>TSIm-2</b> (Figure S23)	<b>S21</b>
<b>17</b>	LDs targeting multifunctional fluorophores (Table S4)	<b>S21-S22</b>
<b>18</b>	Author Contributions	<b>S23</b>
<b>19</b>	Supplementary information references	<b>S23</b>

## 1. General Experimental Details

### 1.1. Synthesis-General Procedures

Unless otherwise stated, all starting materials and reagents were purchased from commercial suppliers and used without further purification. The reactions were monitored using thin-layer chromatography on silica gel 60 F<sub>254</sub> (0.2 mm; Merck). Visualization was accomplished using UV light (254 and 365 nm). Column chromatography was performed on glass columns of different sizes hand-packed with 100-200 mesh silica gel (Merck).

### 1.2. Measurements and Methods

$^1\text{H}$  and  $^{13}\text{C}$  NMR spectra were measured on a 500 MHz Bruker Avance DPX spectrometer using TMS (0 ppm for  $^1\text{H}$  NMR) or  $\text{CDCl}_3$  (77 ppm for  $^{13}\text{C}$  NMR) as an internal reference. Melting points are uncorrected and are determined in open capillary tubes using an electric melting point apparatus. FT-IR spectra were recorded on a Shimadzu IRPrestige-21 Fourier Transform Infrared Spectrophotometer. Electrospray ionization (ESI) high-resolution mass spectra were recorded using Thermo Scientific Exactive mass spectrometer. The electronic absorption spectra were recorded on a Shimadzu spectrophotometer UV-2100. The fluorescence spectra were recorded on a SPEX-Fluorolog-3 FL3-221 spectrofluorimeter. Optical studies in solution-state were carried out in a 1 cm quartz cuvette. SEM images were obtained using Hitachi SU8010 high-resolution field emission scanning electron microscope (SEM) with an accelerating voltage of 10 kV. Samples were prepared by drop casting on a Silicon wafer and dried in air.

#### **1.2.1. Cell Viability Experiment:**

To determine the cytotoxic nature of the **TSIm-1** and **TSIm-2**, colorimetric MTT (3-(4,5-dimethylthiazol-2-yl)-2,5-diphenyltetrazolium bromide) experiment was performed on HeLa cell line. Here, cell suspension of  $5 \times 10^3$  cells/well (100  $\mu\text{L}$ ) were seeded in a 96-well plate and cell lines are grown using DMEM culture media with 10% FBS, 2 mM glutamine and 100 U penicillin / 0.1 mg/mL streptomycin antibiotics for 24 hrs in a  $\text{CO}_2$  incubator. When the cells reached approximately 80% confluency, 100  $\mu\text{L}$  of both the probes at various concentrations (5  $\mu\text{M}$  to 100  $\mu\text{M}$ ) and doxorubicin (1  $\mu\text{M}$ ) were added as a positive control in 96 well plate. The plates were then incubated for 24 h in a 5%  $\text{CO}_2$  incubator. After 24 hrs of incubation, MTT solution in DMEM (0.5 mg/mL) was added to each well and incubation was continued for an additional 2 hrs. The insoluble formazan crystals formed were solubilized by the addition of 100  $\mu\text{L}$  DMSO and the absorbance was measured at 570 nm using a microplate spectrophotometer (BioTek, Synergy H1; MST Lab in SNIoE, Department of Chemistry).

$$\text{Cell Viability (\%)} = \text{Abs. sample/Abs. control} \times 100$$

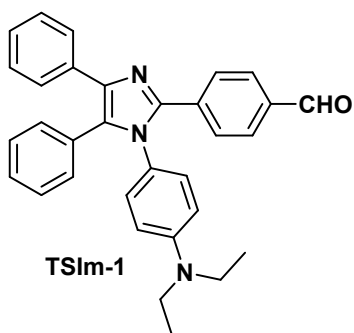
#### **1.2.2. Cellular Co-localization Experiment:**

Co-localization of probes **TSIm-1** and **TSIm-2** was carried out with Nile red, MitoTracker-deep-red and LysoTrackerdeep-red: Prior to imaging, the HeLa cell line

was treated with Nile red (200 nM), MitoTracker-deep red (200 nM), and LysoTracker deep red (200 nM) for 15 minutes, respectively, in serum-free DMEM to label lipid droplets, mitochondria, and lysosomes. Moreover, the cells were co-stained for 30 minutes with the probes, and fluorescence pictures were taken. Pearson's correlation coefficient ( $r$ ) and Mander's overlap coefficients ( $R$ ) were used to determine the degree of co-localization.

## 2. Synthesis and Characterization:

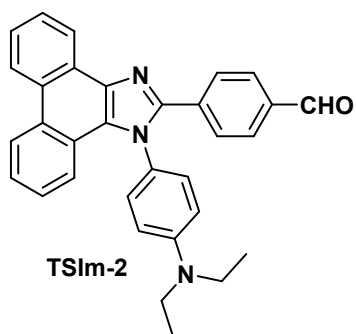
The fluorophores **TSIm-1** and **TSIm-2** were synthesized in a one-step procedure. Structural identification of the intermediates and probe was confirmed by FT-IR,  $^1\text{H}$  NMR,  $^{13}\text{C}$  NMR, and HRMS spectroscopy.



### 2.1. Synthesis of 4-(1-(4-(diethylamino)phenyl)-4,5-diphenyl-1H-imidazol-2-yl)benzaldehyde (**TSIm-1**):

Terephthalaldehyde mono-(diethyl acetal) (1.0 mmol), Benzil (1.0 mmol) were dissolved in glacial acetic acid (5.0 mL) at room temperature. To this solution, 4-Amino-N, N-diethylaniline (3.0 mmol) was added dropwise. After the addition of ammonium acetate (350 mg, 4.5 mmol), the reaction mixture was heated at 110 °C for 24 hrs and the reaction was monitored on TLC. After completion of the reaction, the reaction mixture was cooled to room temperature and poured into the ice water. The precipitate was filtered, washed with cold water, air dried and further, this product was purified by silica gel column chromatography using a gradient of Ethyl acetate and n-Hexane (2/98, v/v) to yield **TSIm-1** (~15 %) as a light green solid.

m.p. 225 °C; FT-IR:  $\nu_{\text{max}}$  = 3061, 2972, 2826, 2736, 1695, 1603, 1570, 1519, 1480, 1448, 1394, 1375, 1356, 1274, 1215, 1200, 1176, 1156, 1133, 1077, 1009, 960, 923, 827, 778, 698  $\text{cm}^{-1}$ ;  $^1\text{H}$  NMR (500.0 MHz,  $\text{CDCl}_3$ , TMS):  $\delta$  = 9.97 (CHO), 7.7 (2H, d), 7.6 (2H, d), 7.5 (2H, d), 7.20 (5H, m), 7.1 (3H, m), 6.8 (2H, d), 6.50 (2H, d), 3.3 (4H, q), 1.1 (6H, t) ppm.  $^{13}\text{C}$  NMR (125.0 MHz  $\text{CDCl}_3$ )  $\delta$  = 12.3, 44.3, 111.5, 124.2, 126.6, 127.3, 127.9, 128.1, 128.2, 128.9, 129.4, 130.6, 131.1, 132.5, 134.4, 135.1, 136.6, 138.7, 145.5, 147.7, 191.9 ppm. HRMS (ESI) m/z:  $[\text{M}+\text{H}]^+$  calcd for  $\text{C}_{32}\text{H}_{30}\text{N}_3\text{O}$  472.2389; found. 472.2384.



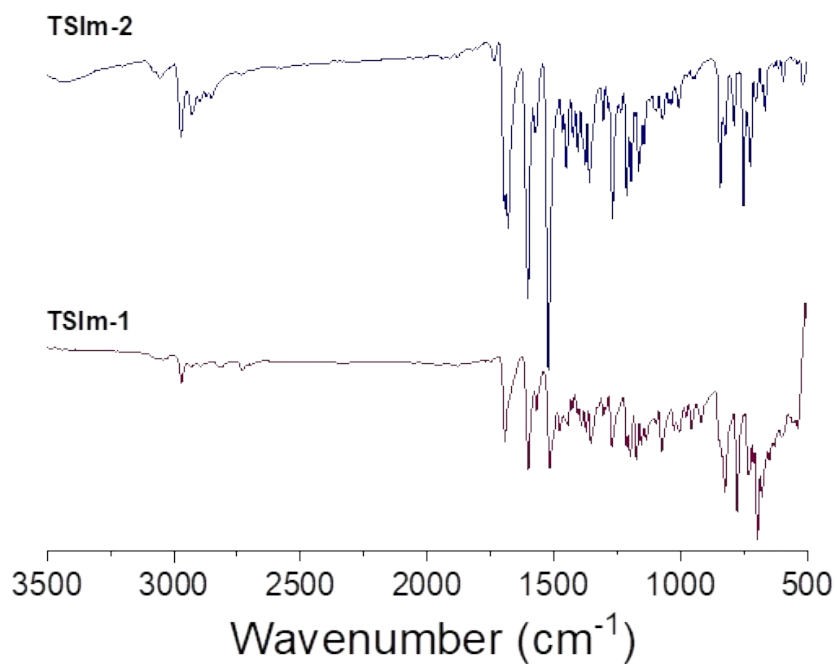
## 2.2. Synthesis of 4-(1-(4-(diethylamino)phenyl)-1H-phenanthro[9,10-d]imidazol-2-yl)benzaldehyde

**(TSIm-2):** Terephthalaldehyde mono-(diethyl acetal) (1.0 mmol), 9,10-Phenanthrenequinone (1.0 mmol) were dissolved in glacial acetic acid (5.0 mL) at room temperature. To this solution, respective 4-Amino-*N,N*-diethylaniline (3.0 mmol) was added dropwise. After

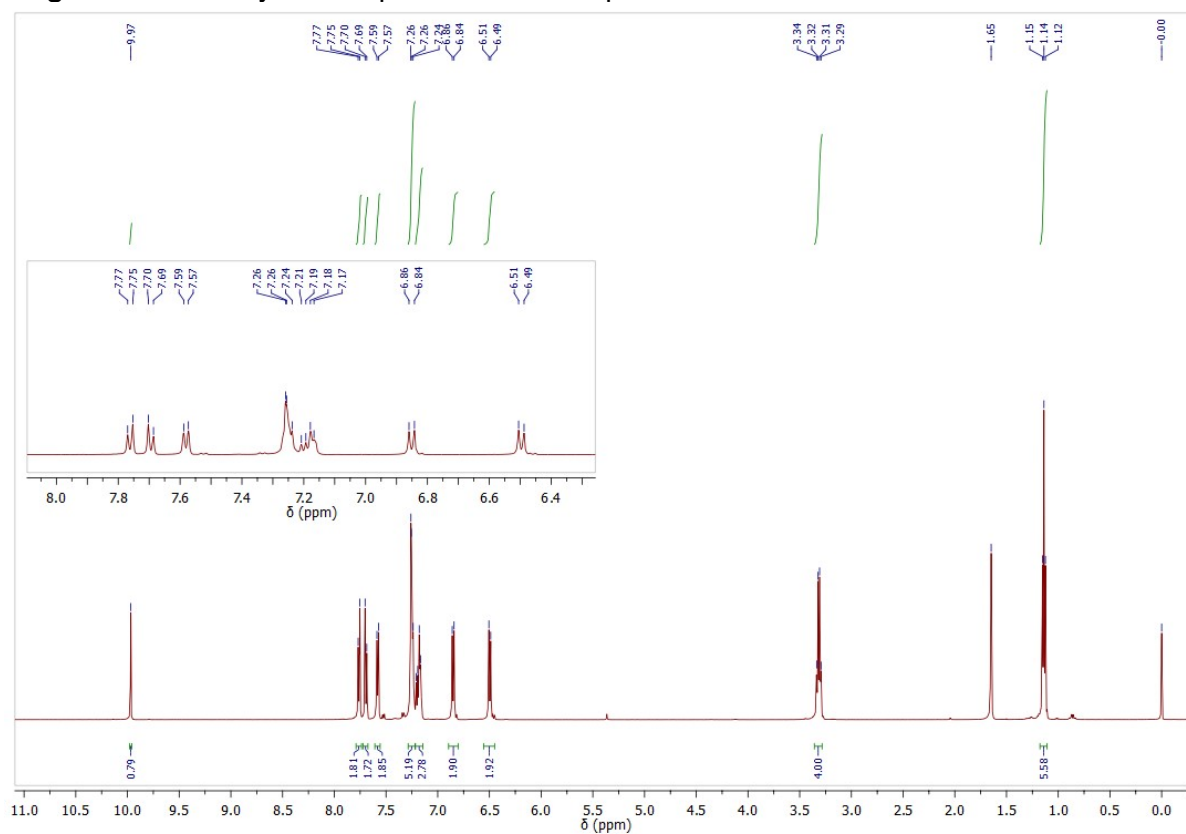
the addition of ammonium acetate (350 mg, 4.5 mmol) the reaction mixture was heated at 110 °C for 24 hrs, and the monitored the reaction on TLC. After completion of the reaction, the reaction mixture was cooled to room temperature and poured into the ice water. The precipitate was filtered, washed with cold water, air dried and further, this product was purified by silica gel column chromatography using gradient of Ethyl acetate and *n*-Hexane (2/98, v/v), to yield **TSIm-2** (~20 %) as light yellow solid.

m.p. 300 °C;  $\nu_{\max}$  = 3064, 2976, 2932, 1740, 1697, 1682, 1604, 1577, 1520, 1469, 1453, 1426, 1407, 1378, 1361, 1308, 1270, 1213, 1196, 1168, 1145, 1074, 1034, 1011, 940, 845, 826, 790, 750, 727, 706, 668, 596, 521  $\text{cm}^{-1}$ ;  $^1\text{H NMR}$  (500.0 MHz,  $\text{CDCl}_3$ , TMS):  $\delta$  = 10.00 (CHO), 8.8 (1H, d), 8.76 (1H, d), 8.70 (1H, d), 7.88 (2H, d), 7.81 (2H, d), 7.74 (1H, t), 7.65 (1H, t), 7.53 (1H, t), 7.46 (1H, d), 7.34 (1H, t), 7.26 (2H, d), 6.79 (2H, d), 3.4 (4H, q), 1.2 (6H, t) ppm.  $^{13}\text{C NMR}$  (125.0 MHz,  $\text{CDCl}_3$ )  $\delta$  = 12.4, 44.5, 112.1, 121.3, 122.6, 123.1, 123.3, 124.0, 125.1, 125.2, 125.7, 126.3, 127.3, 128.3, 129.1, 129.4, 129.4, 129.6, 135.5, 136.7, 137.4, 148.6, 149.5, 191.9 ppm. HRMS (ESI)  $m/z$ :  $[\text{M}+\text{H}]^+$  calcd for.  $\text{C}_{32}\text{H}_{28}\text{N}_3\text{O}$  470.2232, obs. 470.2251.

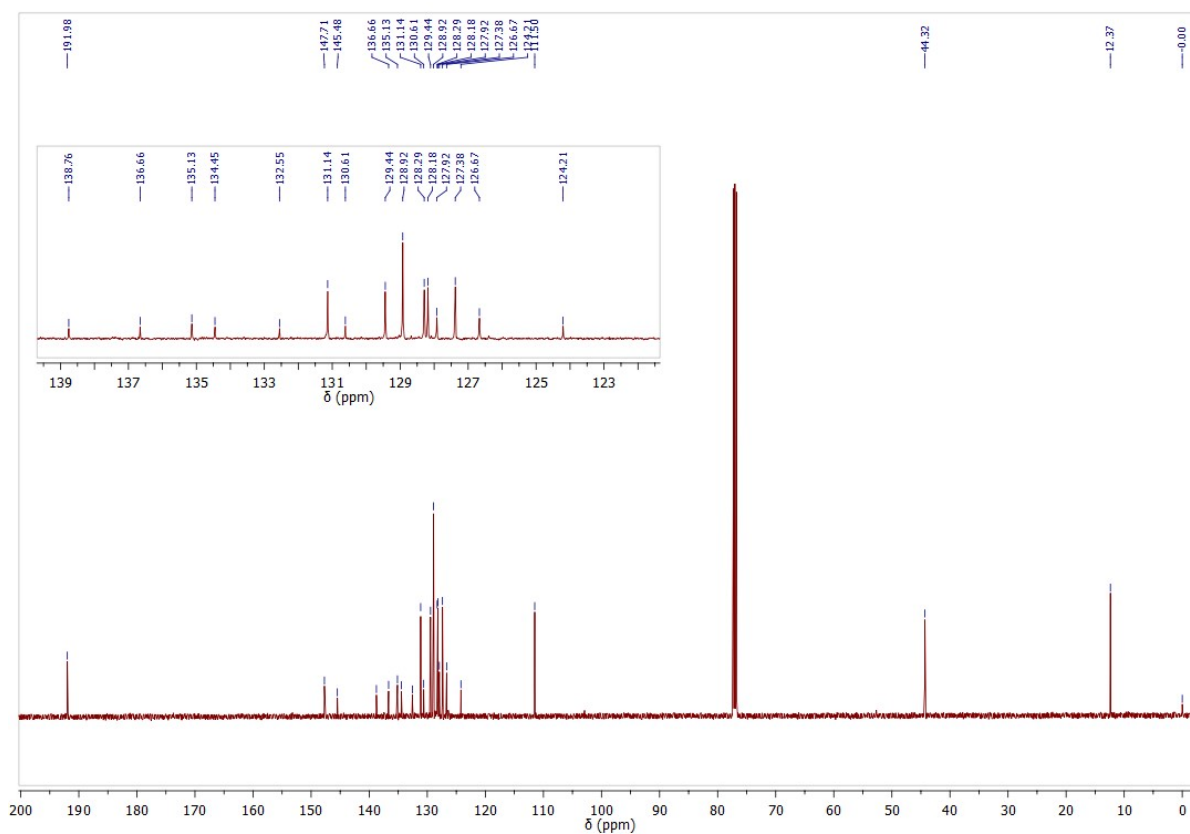
## 3. FT-IR, $^1\text{H NMR}$ , $^{13}\text{C NMR}$ , and HRMS Spectra of TSIm-1 and TSIm - 2



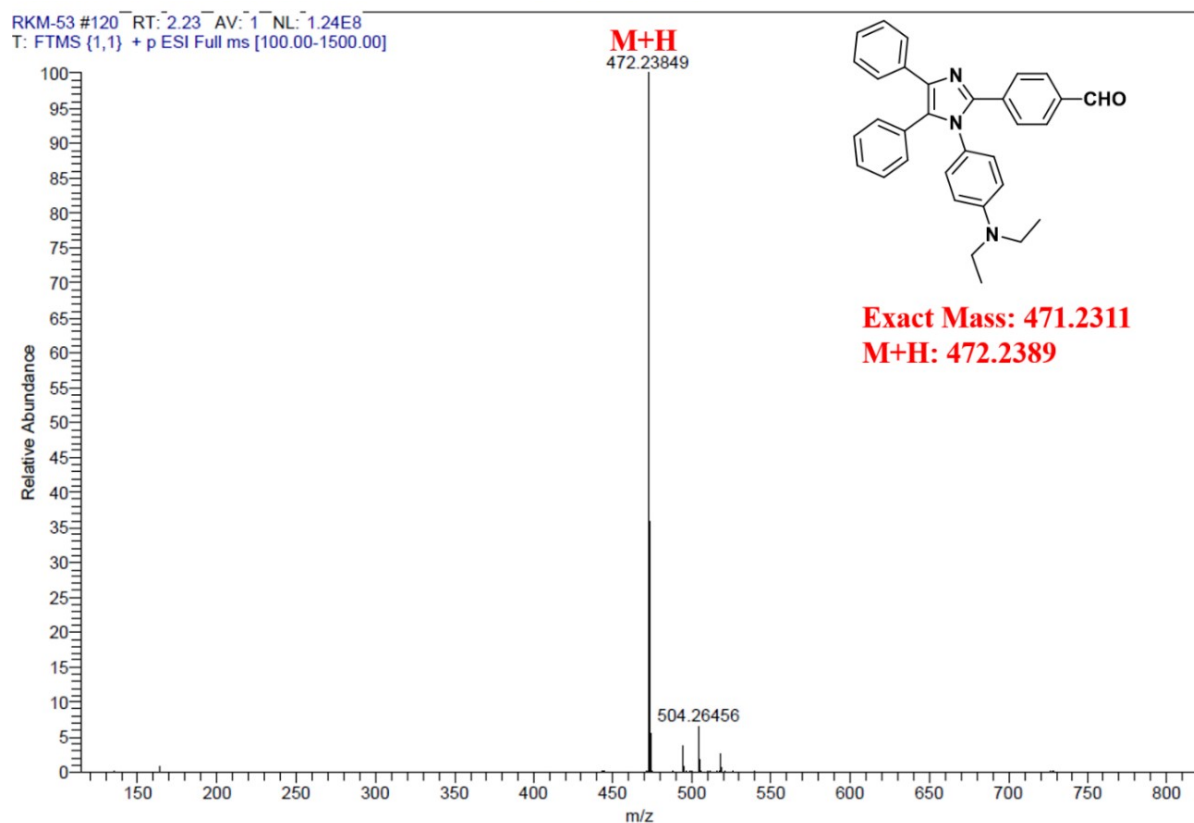
**Figure S1:** Overlay FT-IR spectra of the compounds **TSIIm-1** and **TSIIm-2**.



**Figure S2:**  $^1\text{H}$  NMR (500 MHz) spectrum of **TSIIm-1** in  $\text{CDCl}_3$ .

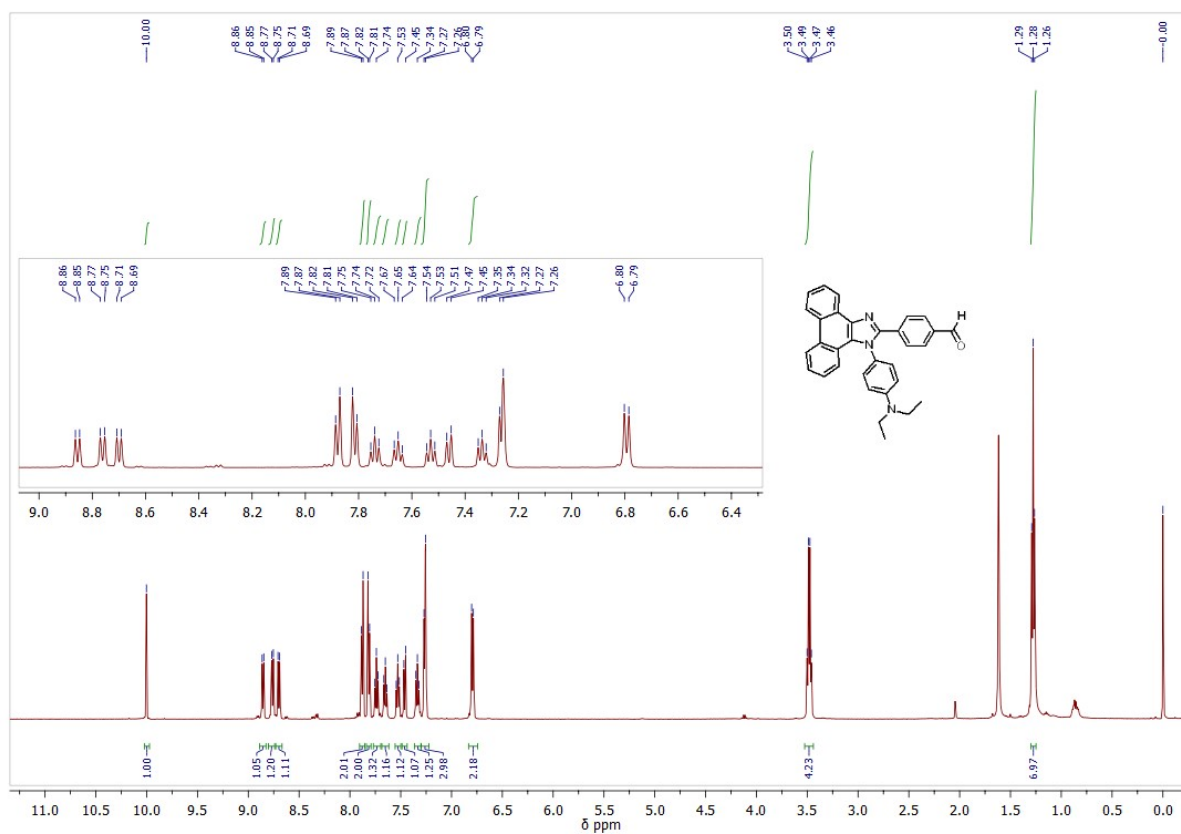


**Figure S3:**  $^{13}\text{C}$  NMR (125 MHz) spectrum of compound **TSIm-1** in  $\text{CDCl}_3$ .

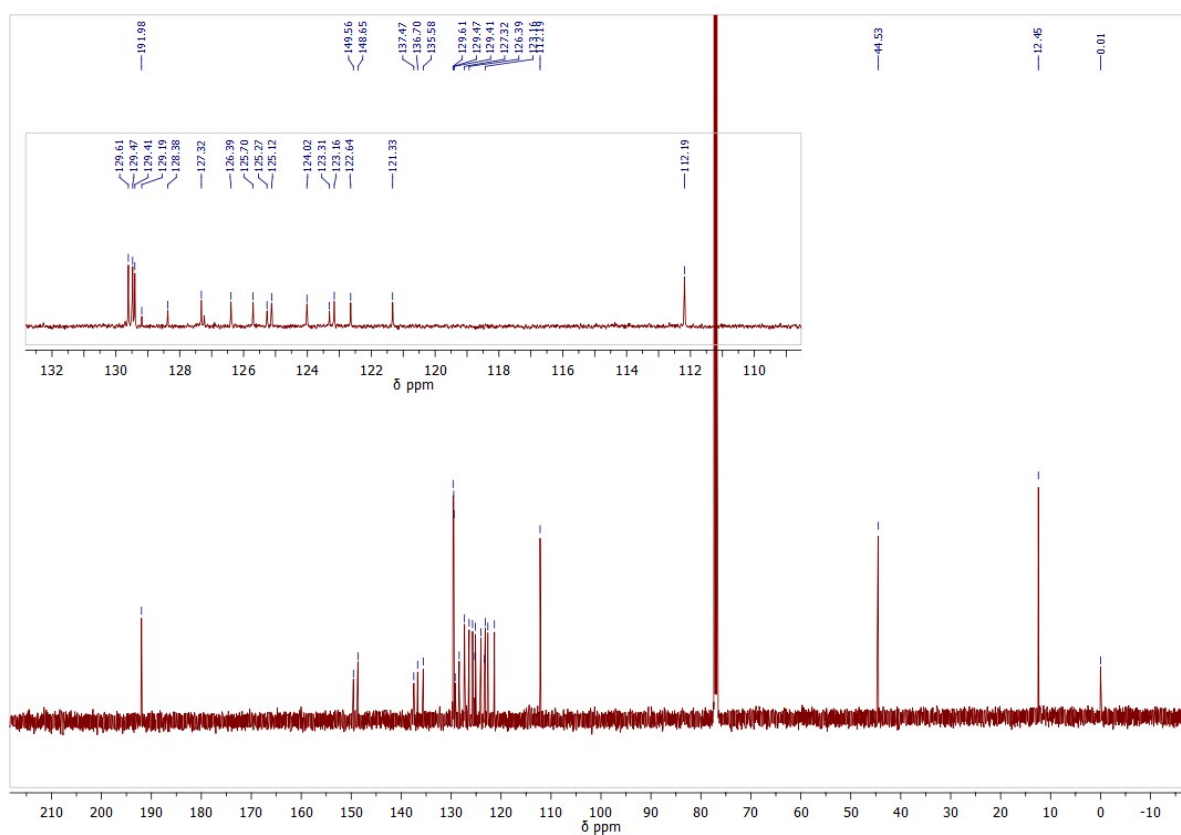


**Figure S4:** HRMS spectrum of compound **TSIm-1**.

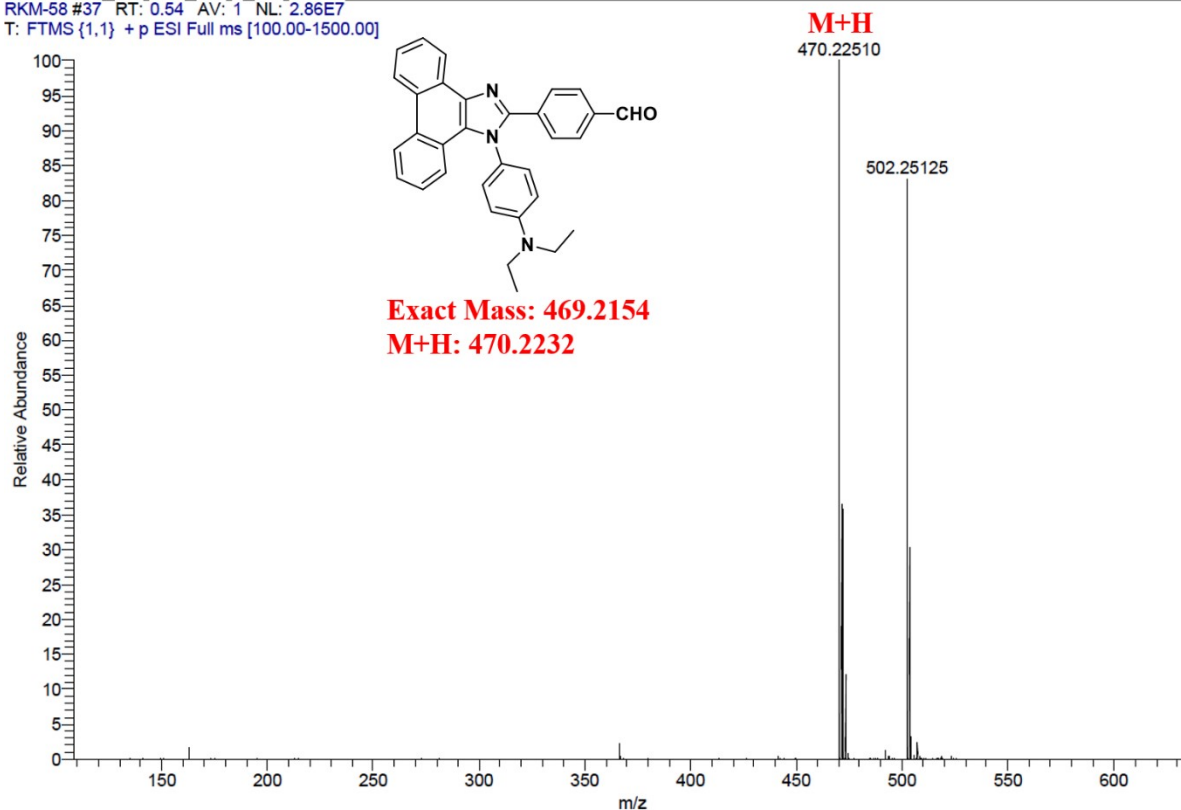




**Figure S5:**  $^1\text{H}$  NMR (500 MHz) spectrum of compound **TSIm-2** in  $\text{CDCl}_3$ .



**Figure S6:**  $^{13}\text{C}$  NMR (125 MHz) spectrum of compound **TSIm-2** in  $\text{CDCl}_3$ .

RKM-58 #37 RT: 0.54 AV: 1 NL: 2.86E7  
T: FTMS (1,1) + p ESI Full ms [100.00-1500.00]

**Figure S7:** HRMS spectrum of compound **TSIm-2**

#### 4. Theoretical Studies of **TSIm-1** & **TSIm-2**:

For the determination of the electronic behaviour of the probe **TSIm-1** and **TSIm-2** in the absence and presence of solvent, we performed DFT calculation by using the Gaussian 16 program and Gauss View 6.0 as a visualization program. The probe **TSIm-1** and **TSIm-2** in the gaseous phase were optimized by using the B3LYP exchange functional retaining 6-31+G(d,p) basis set.<sup>S18-S22</sup> Consequently, for the understanding of the absorption properties of the probe, we performed the time-dependent density functional theory (TDDFT). It is observed that the HOMO of probe **TSIm-1** and **TSIm-2** is distributed over imidazole and benzaldehyde moiety while LUMO is located at the benzaldehyde unit. This electron redistribution from the electron-donating moiety to the electron-withdrawing moiety showed a similar pattern in the S<sub>0</sub>-S<sub>1</sub> transitions (HOMO-LUMO), which indicated the intramolecular charge transfer behaviour. It is well established that the higher dipole moment of a molecule in the excited state also processes higher polarity than in the ground state, which imposes a large effect of solvent polarity on the excited state.

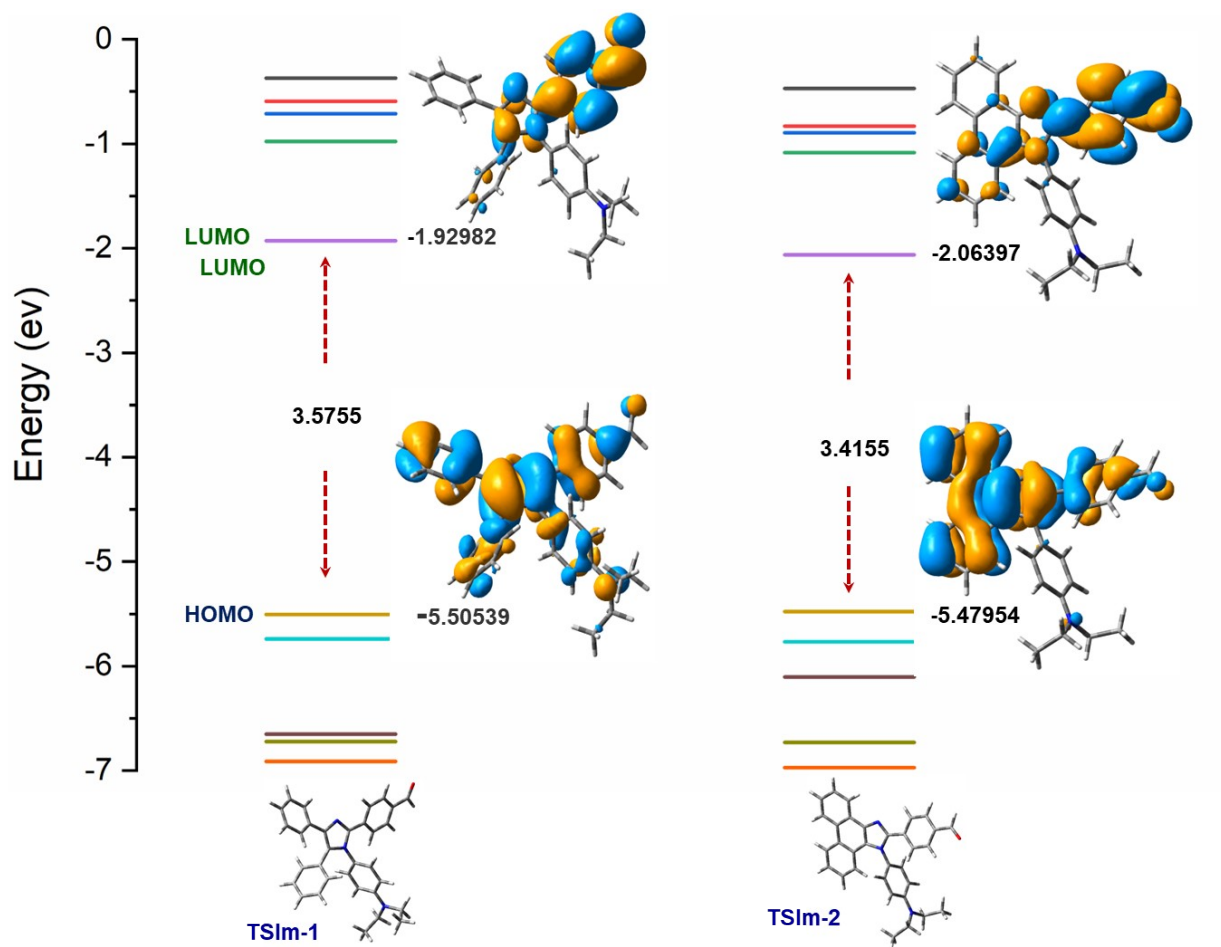


**Figure S8:** Energy calculation of frontier molecular orbital HOMO & LUMO of the **TSIm-1** and **TSIm-2**.

## 5.1. Photophysical properties of TSIm-1 and TSIm-2 in solid state:

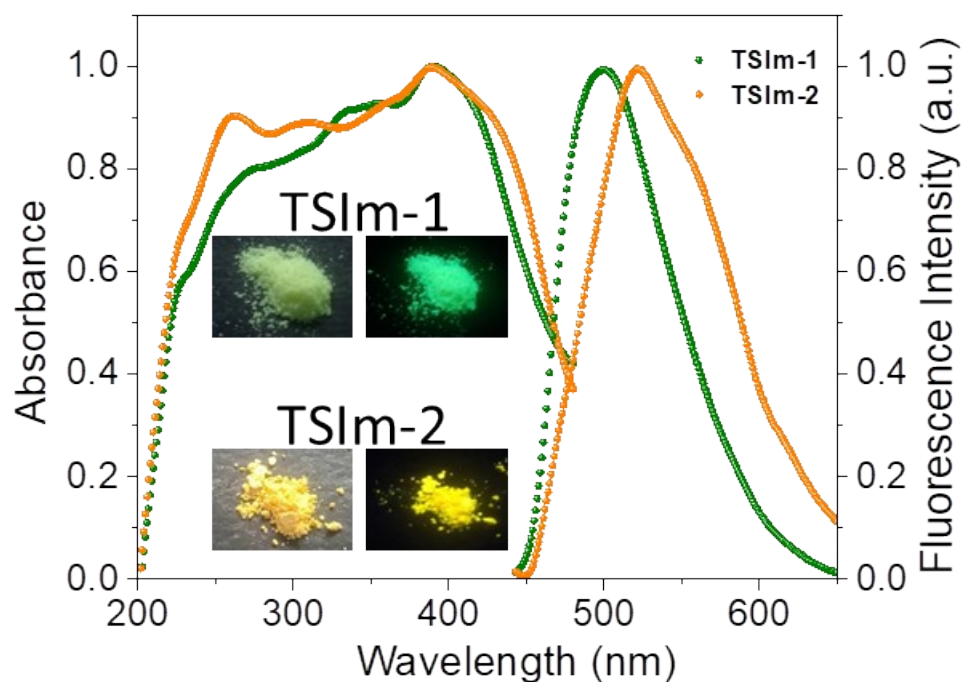


**Figure S9:** Solid states absorption and luminescence behaviour of **TSIm-1** and **TSIm-2**.

## 5.2. Absorption spectra of TSIm-1 and TSIm-2

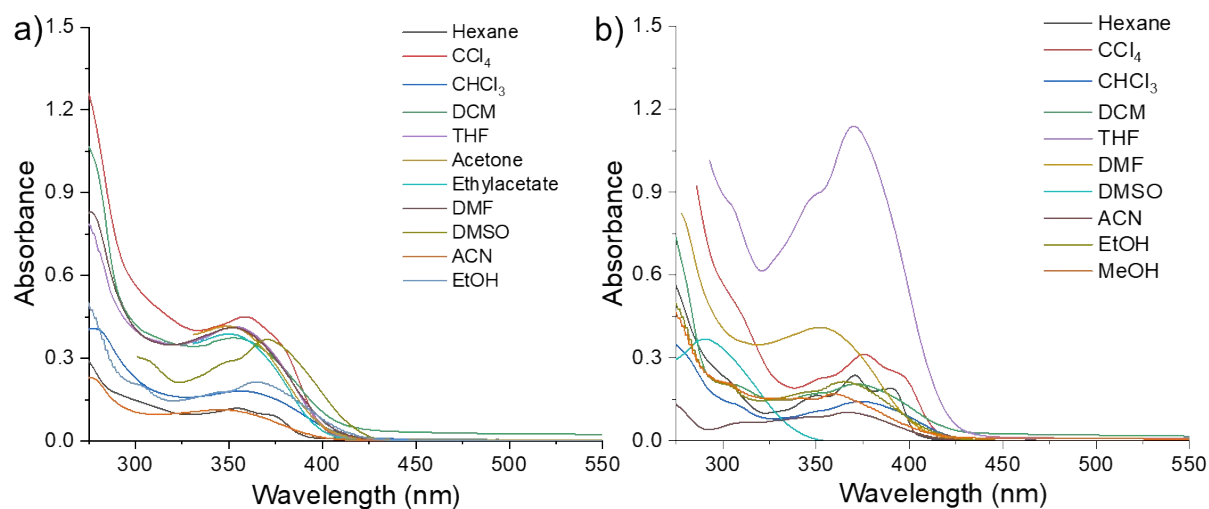


**Figure S10:** Absorption spectra of a) **TSIm-1** (15  $\mu\text{M}$ ); and b) **TSIm-2** (10  $\mu\text{M}$ ) in different solvents.

## 6. Demonstration of TICT process:

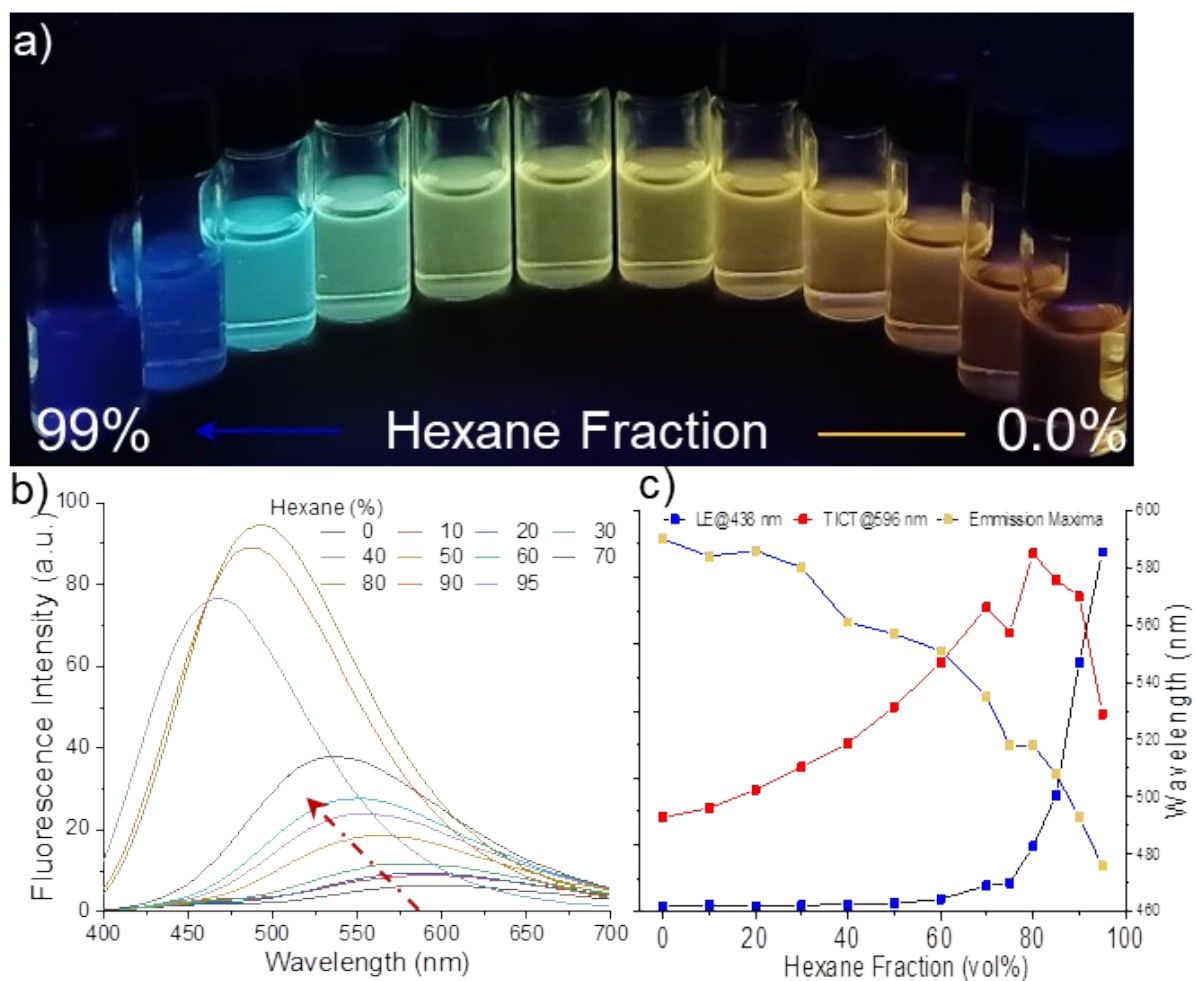


**Figure S11.** a) Photographs of **TSIIm-1** in DCM/hexane mixtures (15  $\mu\text{M}$ ) with different fractions of hexane ( $f_h$ ) taken under UV illumination. (b) Emission spectra of **TSIIm-1** in different DCM/hexane mixtures. (c) Plots of maximum emission intensity ( $I$ ) and wavelength ( $\lambda_{em}$ ) of **TSIIm-1** versus hexane fraction ( $f_h$ ) in the DCM/hexane mixture. Solution concentration: 10  $\mu\text{M}$ . Excitation wavelength: 380 nm.

## 7. Aggregation studies of TSIm-1 and TSIm-2

The AIE properties of TSIm-1 and TSIm-2 were investigated by measuring their photoluminescence spectra in THF, DMSO, and ACN/water mixtures.

### 7.1. Aggregation studies of TSIm-1 and TSIm-2 in THF/Water mixture.

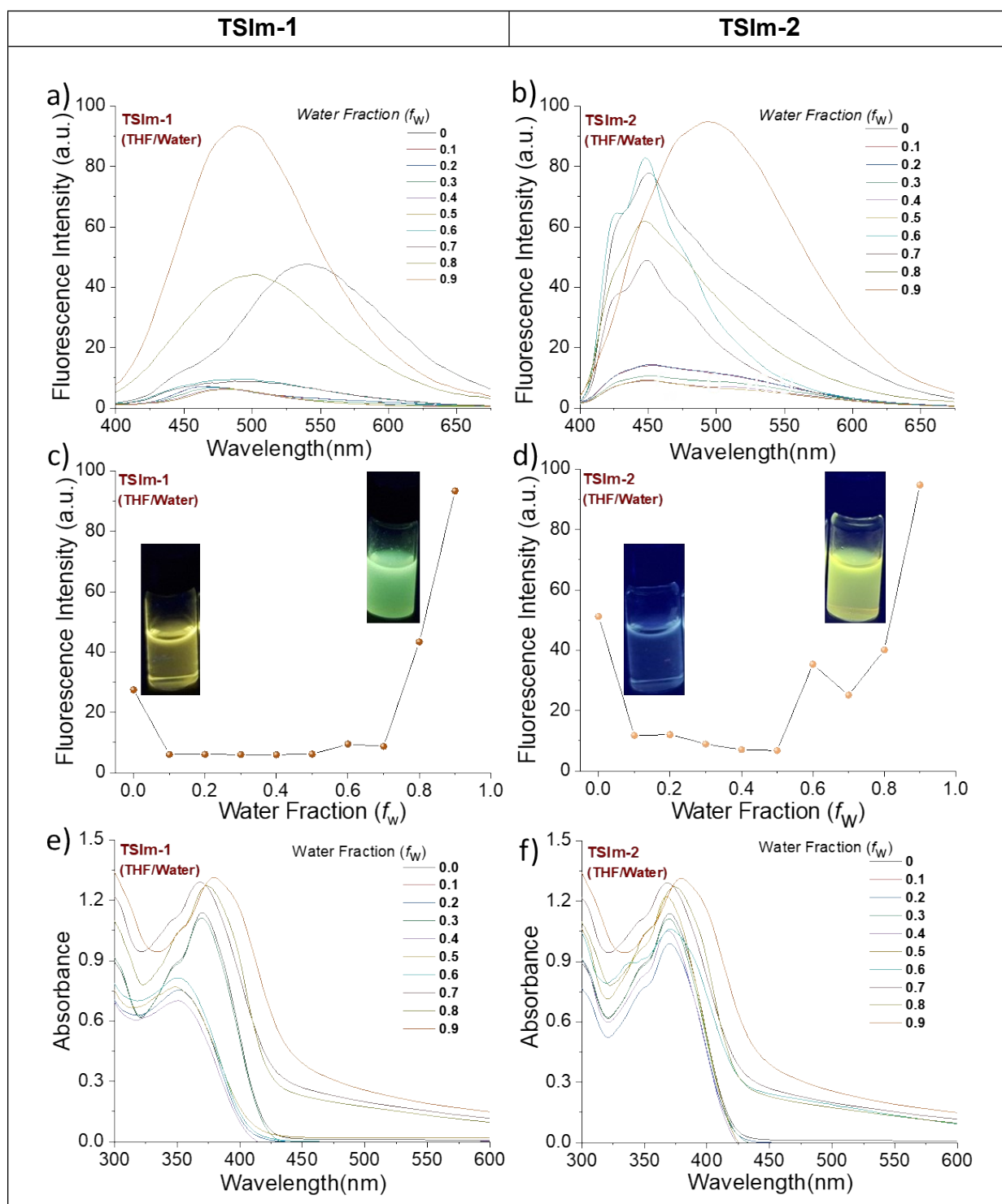


**Figure S12:** Fluorescence spectra (10  $\mu\text{M}$ ,  $\lambda_{\text{ex}} = 370 \text{ nm}$ ) of a) **TSIm-1** (15  $\mu\text{M}$ ) and b) **TSIm-2** (10  $\mu\text{M}$ ) in different THF-water fractions (0 $\rightarrow$ 0.9). The fluorescence intensities of c) **TSIm-1** and d) **TSIm-2** at 510 nm, respectively. Corresponding absorption of e) **TSIm-1** and f) **TSIm-2**.

**7.2: Aggregation studies of TSIm-1 and TSIm-2 in DMSO/Water mixture.**

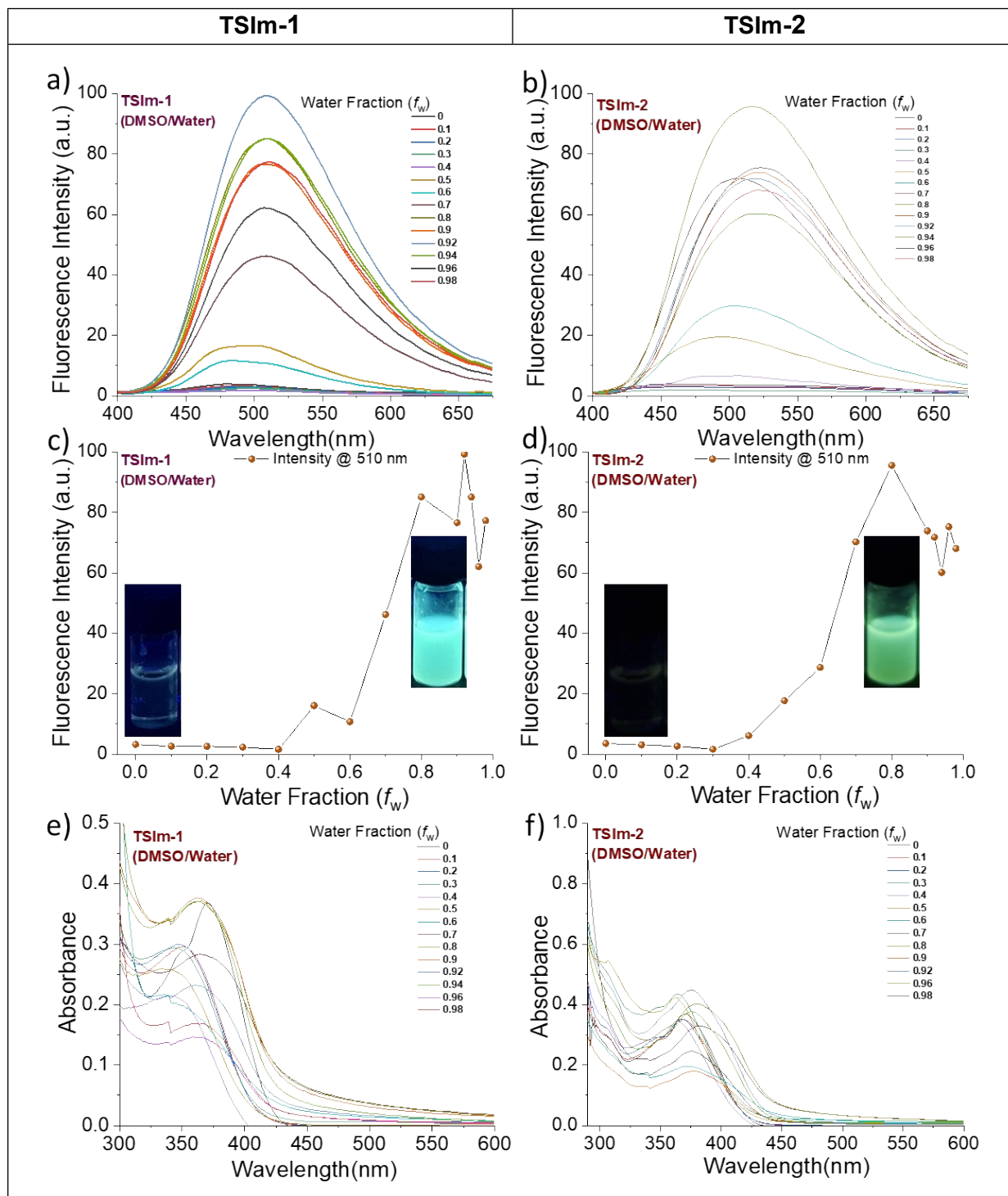


**Figure S13:** Fluorescence spectra (10  $\mu\text{M}$ ,  $\lambda_{\text{ex}} = 370 \text{ nm}$ ) of a) **TSIm-1** and b) **TSIm-2** in different DMSO-water fractions (0 $\rightarrow$ 0.9). The fluorescence intensities of c) **TSIm-1** and d) **TSIm-2** at 510 nm, respectively. Corresponding absorption of e) **TSIm-1** and f) **TSIm-2**.

### 7.3. Aggregation studies of TSIIm-1 and TSIIm-2 in ACN/Water mixture.

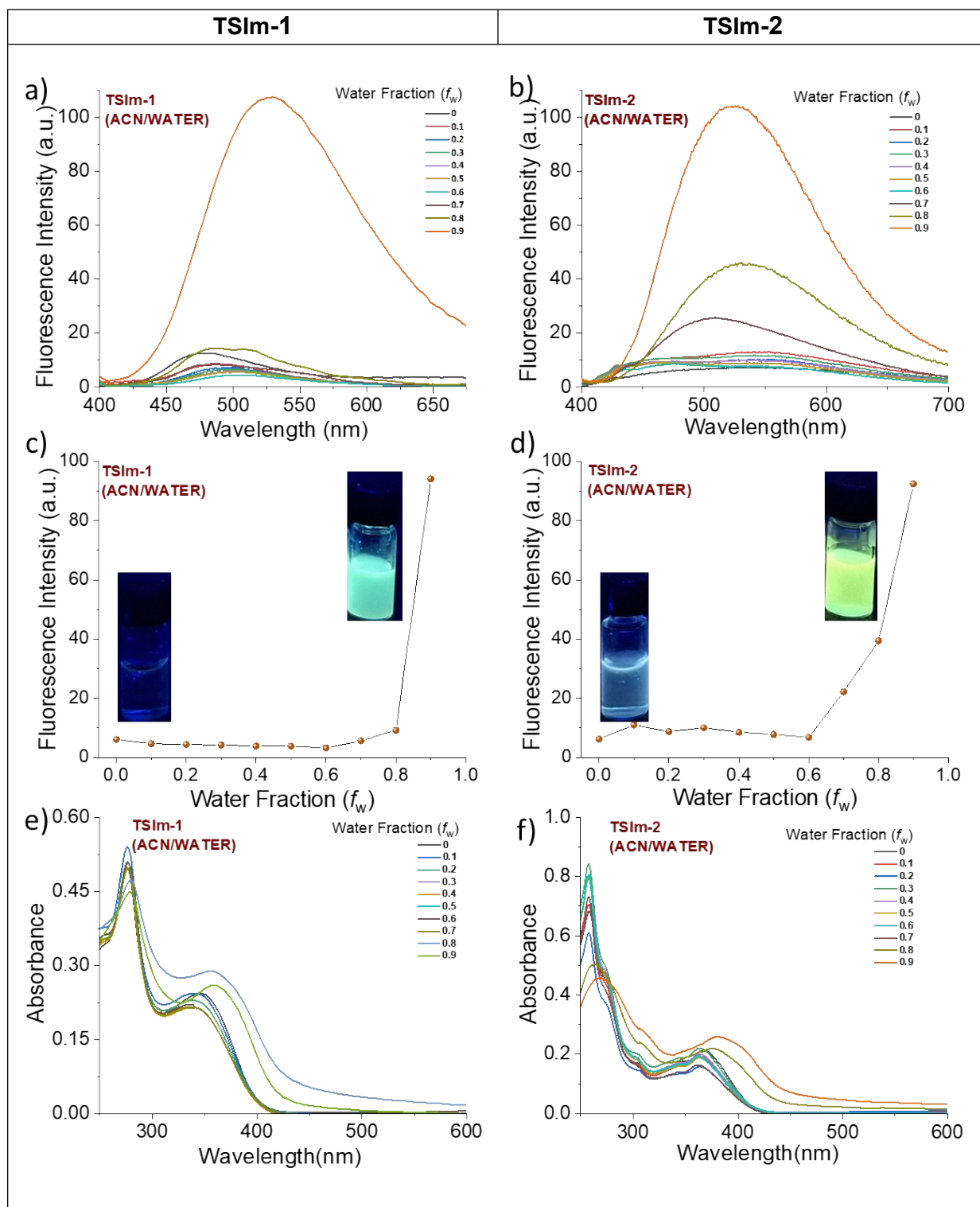


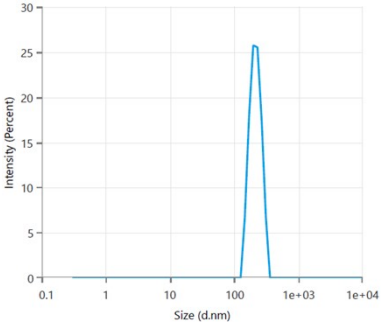
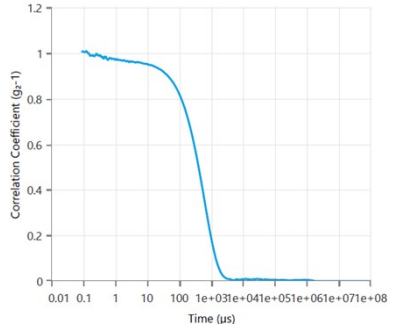
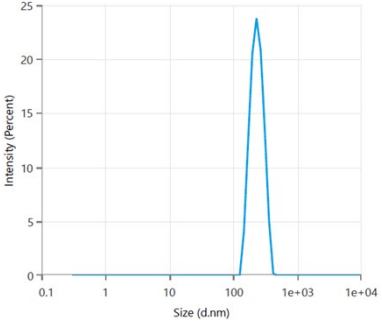
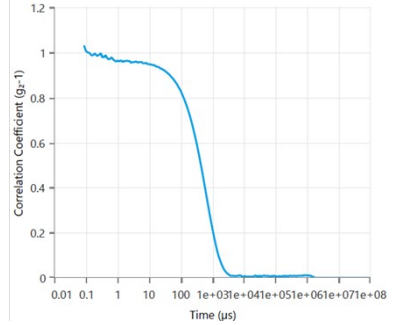
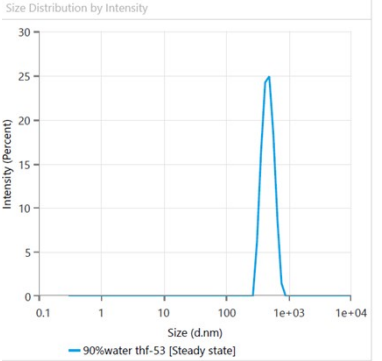
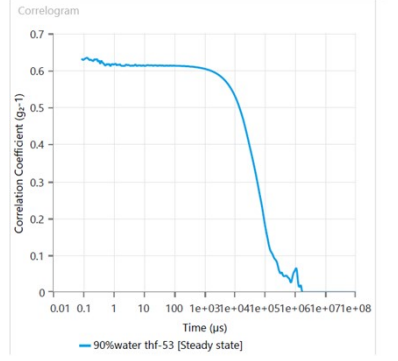
**Figure S14:** Fluorescence spectra (10  $\mu$ M,  $\lambda_{\text{ex}} = 370$  nm) of a) TSIIm-1 and b) TSIIm-2 in different ACN-water fractions (0 $\rightarrow$ 0.9). The fluorescence intensities of c) TSIIm-1 and d)



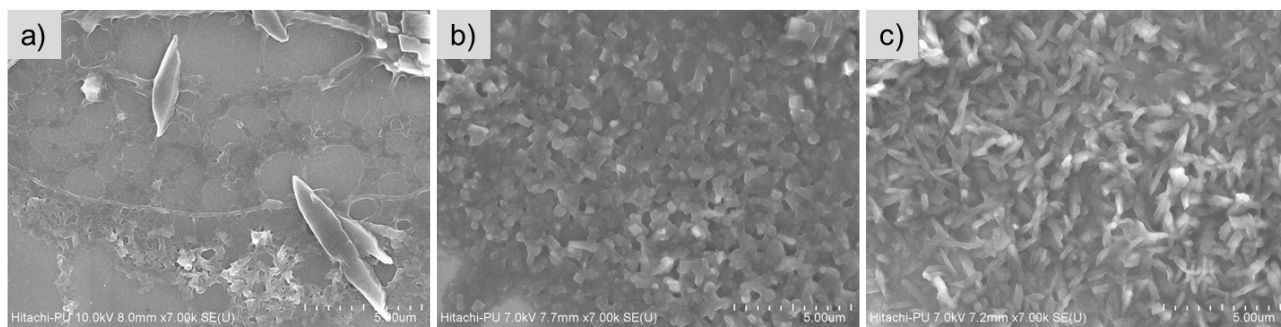
TSIm-2 at 510 nm, respectively. Corresponding absorption of e) TSIm-1 and f) TSIm-2.

## 8. Dynamic Light Scattering (DLS) and SEM studies TSIm-1<sub>Agg</sub> and TSIm-2<sub>Agg</sub>

### 8.1. Table S1. DLS data of TSIm-1 in organic solvent (90% H<sub>2</sub>O fraction)

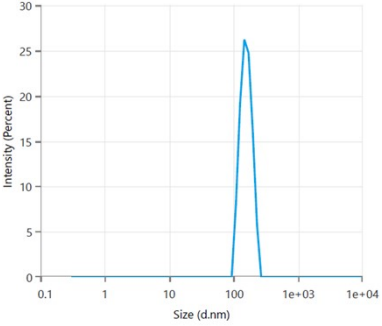
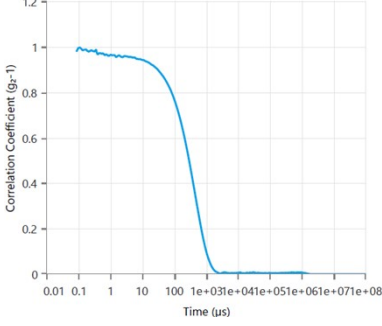
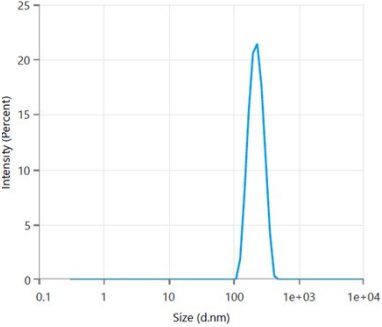
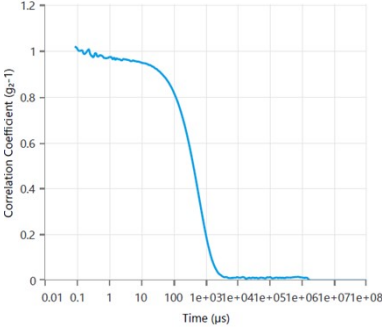
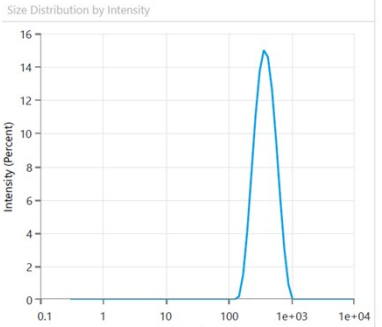
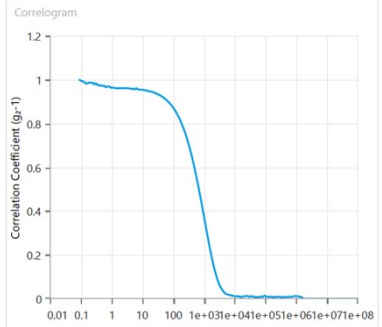
TSIm-1			
Solvent Composition	Z-Average (nm)	Size Distribution by Intensity	Correlogram
DMSO-H <sub>2</sub> O (90%)	210.8		
ACN-H <sub>2</sub> O (90%)	226.1		
THF-H <sub>2</sub> O (90%)	476		

### 8.2. SEM images of TSIm-1<sub>Agg</sub>



**Figure S15:** SEM image of the **TSIm-1<sub>Agg</sub>** (a-c) in different solvent conditions. a) DMSO-Water ( $f_w=0.9$ ); b) ACN-Water ( $f_w=0.9$ ) and c) THF-Water ( $f_w=0.9$ ) mixture.

### 8.3. Table S2: DLS data of TSI<sub>m</sub>-2 with organic solvent (90% H<sub>2</sub>O fraction)

TSI <sub>m</sub> -2			
Solvent Composition	Z-Average(nm)	Size Distribution by Intensity	Correlogram
DMSO-H <sub>2</sub> O (90%)	154.1		
ACN-H <sub>2</sub> O (90%)	212.9		
THF-H <sub>2</sub> O (90%)	345.6		

### 8.4. SEM images of TSI<sub>m</sub>-2<sub>Agg</sub>

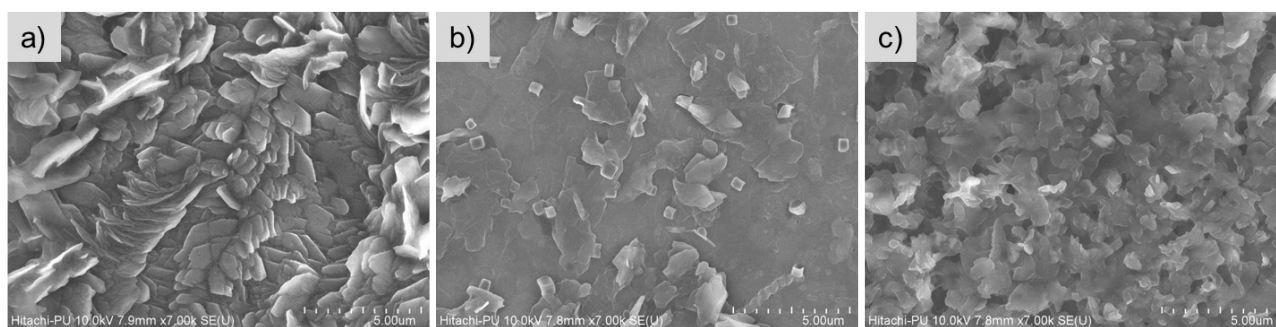


**Figure S16:** SEM image of the TSI<sub>m</sub>-2<sub>Agg</sub> (a-c) in different solvent conditions. a) DMSO-Water ( $f_w=0.9$ ); b) ACN-Water ( $f_w=0.9$ ) and c) THF –Water ( $f_w=0.9$ ) mixture.

## 9. <sup>1</sup>H NMR studies of TSIIm-1 with D<sub>2</sub>O

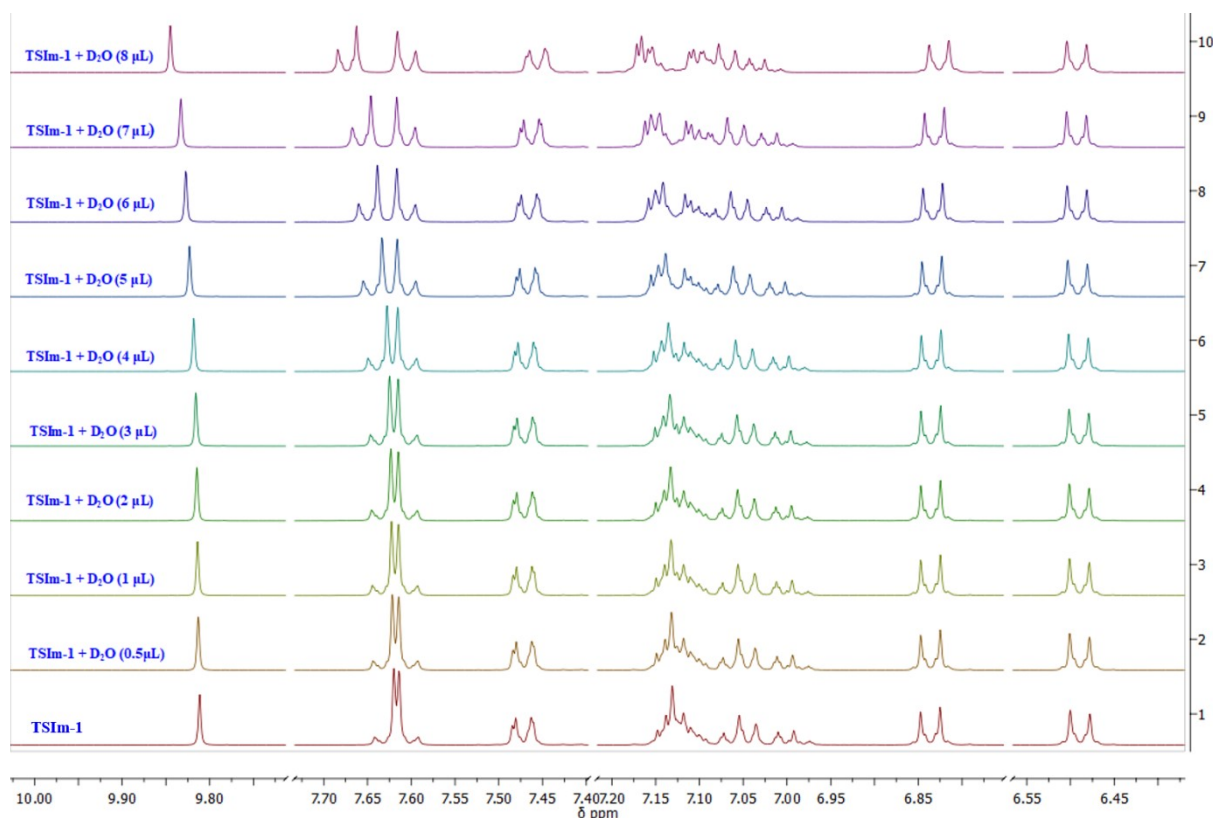
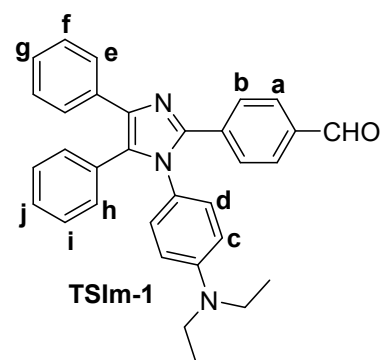


**Figure S17:** <sup>1</sup>H NMR Studies of TSIIm-1 in Tetrahydrofuran-d<sub>8</sub> (THF-d<sub>8</sub>) in the presence of different D<sub>2</sub>O fractions.

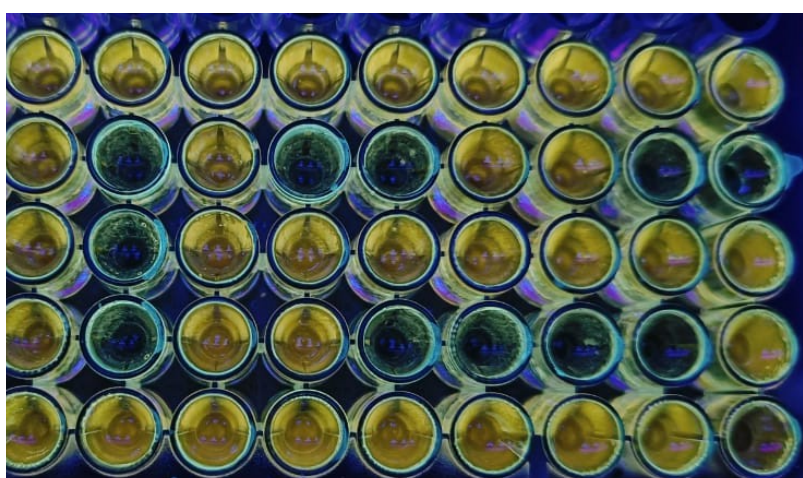
### 9.1. Table S3. <sup>1</sup>H NMR titration studies of TSIIm-1 with different D<sub>2</sub>O concentration

Species	Protons					
	-CHO	H <sub>a</sub>	H <sub>b</sub>	H <sub>h</sub>	H <sub>f</sub>	H <sub>c</sub>
TSIIm-1 + D <sub>2</sub> O						
TSIIm-1 + D <sub>2</sub> O (0.0 μL)	9.811	7.631	7.606	7.478	6.836	6.489
TSIIm-1 + D <sub>2</sub> O (0.5 μL)	9.813	7.633	7.603	7.476	6.836	6.489
TSIIm-1 + D <sub>2</sub> O (1.0 μL)	9.814	7.634	7.604	7.476	6.836	6.49
TSIIm-1 + D <sub>2</sub> O (2.0 μL)	9.815	7.634	7.604	7.470	6.835	6.49
TSIIm-1 + D <sub>2</sub> O (3.0 μL)	9.816	7.635	7.604	7.47	6.835	6.49
TSIIm-1 + D <sub>2</sub> O (4.0 μL)	9.818	7.638	7.604	7.469	6.835	6.491
TSIIm-1 + D <sub>2</sub> O (5.0 μL)	9.823	7.644	7.605	7.467	6.834	6.492
TSIIm-1 + D <sub>2</sub> O (6.0 μL)	9.827	7.649	7.605	7.465	6.833	6.492
TSIIm-1 + D <sub>2</sub> O (7.0 μL)	9.833	7.657	7.606	7.462	6.831	6.493
TSIIm-1 + D <sub>2</sub> O (8.0 μL)	9.845	7.678	7.605	7.456	6.826	6.493



## 10. Imaging pattern obtained by TSIm-1 triggered by different trace water input

a  
)



b  
)

19033	19098	18518	27287	19043	18922	18445	19069	18617	19715	18843	19504
6005	6045	18293	18534	6144	18487	6519	6142	18579	18631	5955	6028
17949	18210	19111	18738	6547	18203	18636	18276	18111	18556	19292	18964
18890	7692	7358	18696	6776	18670	18294	6593	6741	6693	6287	18719
19231	18520	17120	19492	18645	18970	17906	18055	19225	18043	18644	18418

**Figure S18:** a) Fluorescence intensity pattern of TSIm-1 (450  $\mu$ M, THF) in a 96-well plate triggered by different trace water input (0.1% water-THF); b) Fluorescence intensity recorded by the BioTek SynergyH1 microplate reader (25  $\mu$ M, THF and 0.1water-THF,  $\lambda_{ex}$  = 380 nm,  $\lambda_{em}$  = 530 nm).

## 11. Trace water detection properties of TSIm-2

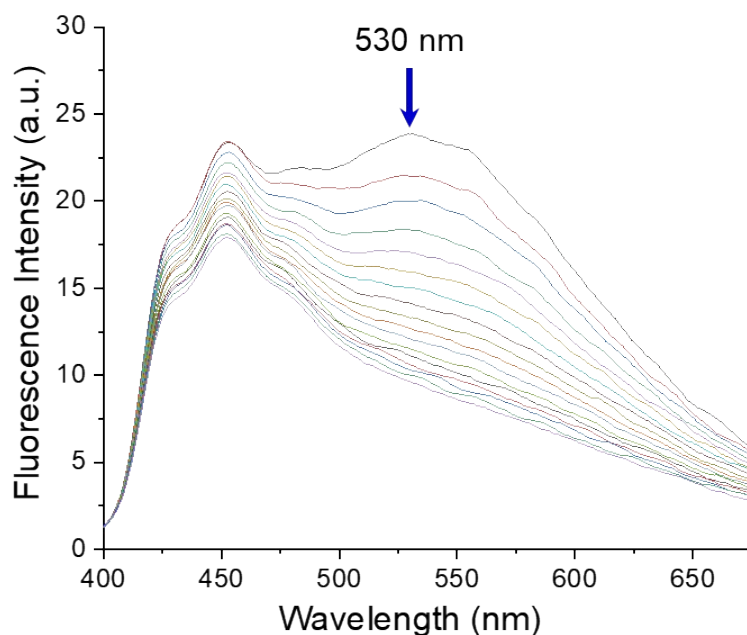


**Figure S19:** Change in fluorescence intensity of **TSIIm-2** (10  $\mu\text{M}$ ,  $\lambda_{\text{ex}} = 380 \text{ nm}$ ) with increasing water percentage (0-1.7, v/v %).

## 12. Photostability studies of TSIIm-1 and TSIIm-2

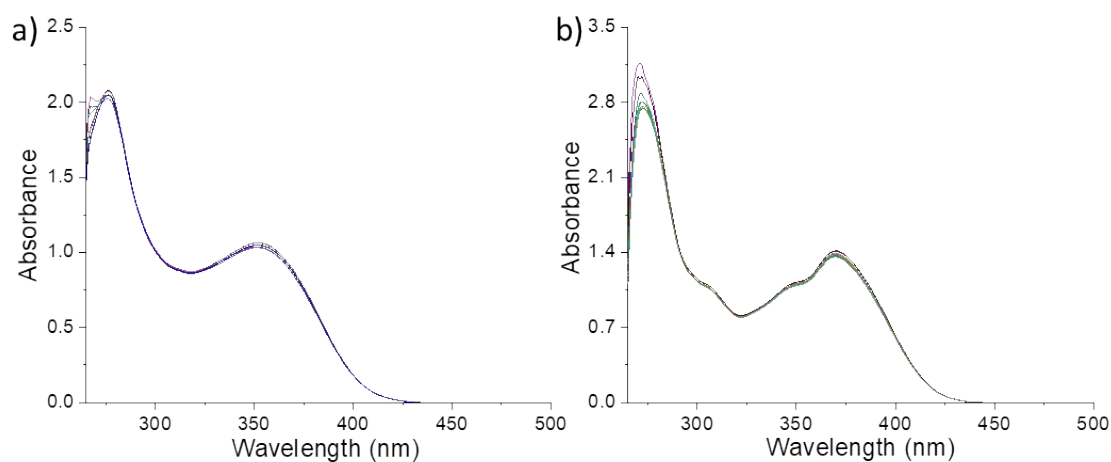


**Figure S20:** UV/vis spectra of a) **TSIIm-1** (18  $\mu\text{M}$ ) and b) **TSIIm-2** (12  $\mu\text{M}$ ) on radiation by a 300 W xenon lamp for 35 min using 375nm filter.

## 13. Cytotoxicity studies of TSIIm-1 and TSIIm-2 in HeLa cell line

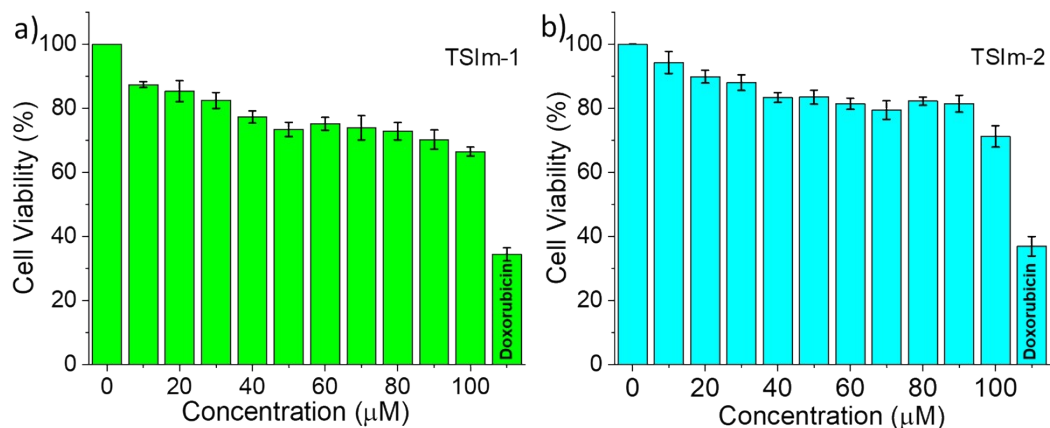


**Figure S21:** In vitro cytotoxicity in HeLa cells treated with a) TSI-1 and b) TSI-2 at different concentrations.

#### 14. Cytotoxicity studies of TSI-1 and TSI-2 in HepG2 cell line

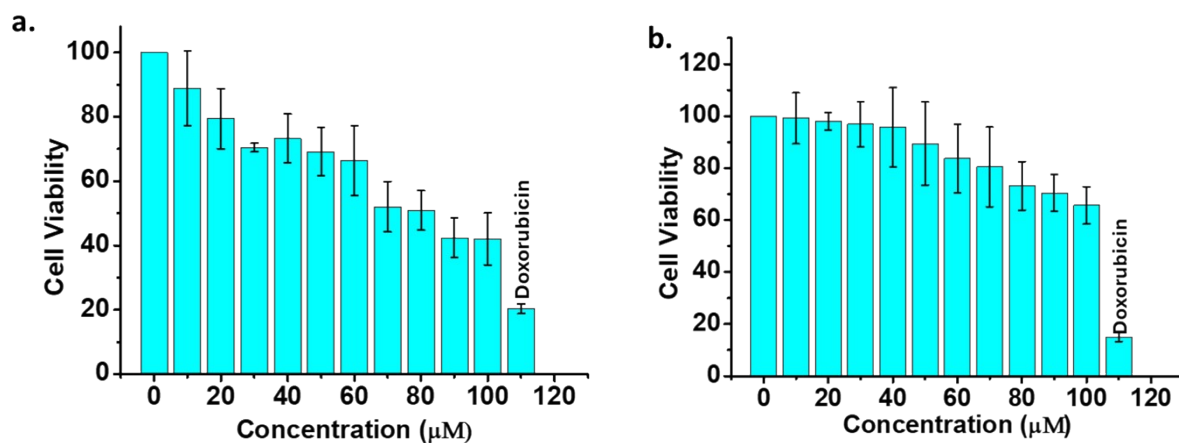


**Figure S22:** MTT assay of a) TSI-1 and b) TSI-2 in HepG2 cell line.

#### 15. Fluorescence imaging with TSI-2 and response without/with oleic Acid

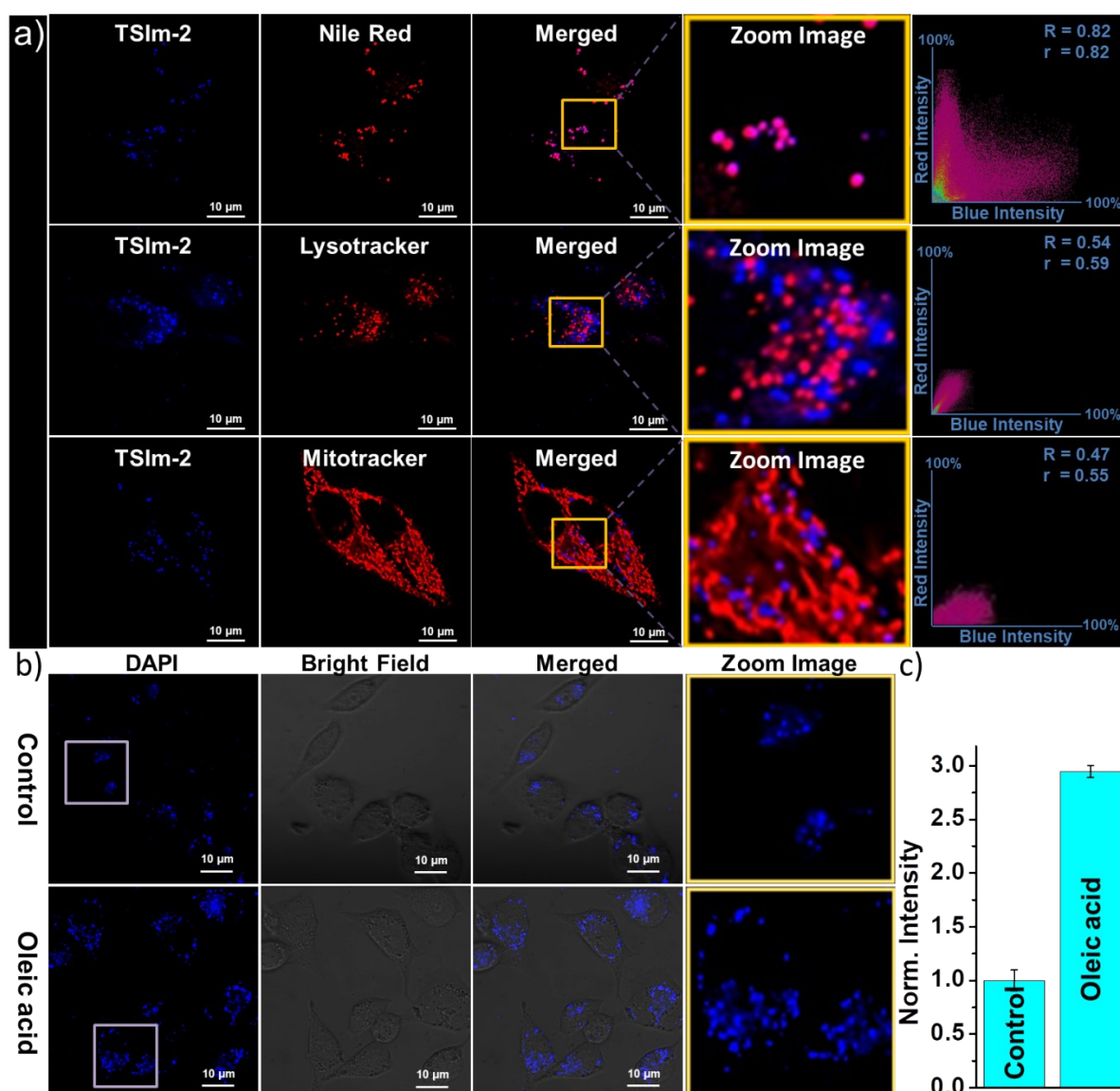


**Figure S23:** a) Confocal fluorescence images for intracellular localization of **TSIm-1** (40 μM) in the blue channel ( $\lambda_{ex} = 404$  nm,  $\lambda_{em} = 425-475$  nm) after administration in HeLa cells for 30 min. Images were acquired after counter-staining in the red channel ( $\lambda_{em} = 580-620$  nm) for the Nile red (200 nM;  $\lambda_{ex} = 560$  nm), deep-red channel ( $\lambda_{em} = 650-720$  nm) for MitoTracker deep red (200 nM;  $\lambda_{ex} = 640$  nm) and LysoTracker deep red (200 nM;  $\lambda_{ex} = 640$  nm). The corresponding 'r' and 'R' represent Pearson's correlation coefficient and Mander's overlap coefficient, respectively. Images were captured using a 100 oil emersion lens with 2X zoom. b) The cells were incubated with **TSIm-2** (40 μM) for 30 min after the cells were stimulated without/with oleic acid at 37 °C for 4 h. Images were acquired in a confocal microscope. The image scale bar is 10 μm. Images were captured using a 60 oil emersion lens with 2 X zoom; c) Bar graph showing normalized fluorescence intensity of the cells without/with oleic acid.



## 16. Monitoring of LDs generation in HepG2 cells with TSIIm-2 via flow cytometry

The results obtained from flow cytometry analysis following oleic acid treatment indicated a significant increase in LDs, accompanied by enhanced fluorescence intensity in oleic acid (300  $\mu\text{M}$ ) treated cells, achieving  $\sim 42.57\%$ , compared to the control group ( $\sim 22.19\%$ ) and thus further supporting our claim that our probes are able to monitor LDs effectively in the cells.

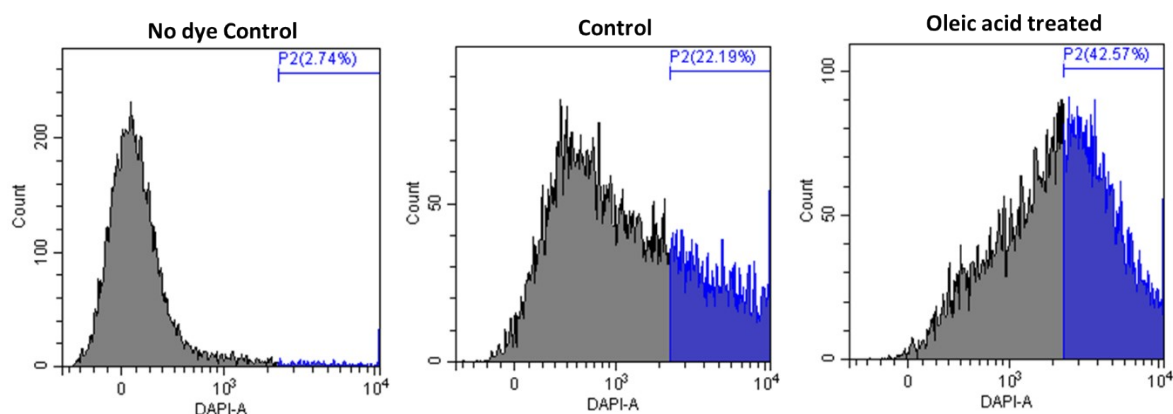


**Figure S24:** Monitoring of LDs generation in HepG2 cells via flow cytometry with TSIIm-2 (80  $\mu\text{M}$ ) in response to oleic acid treatment (300  $\mu\text{M}$ ) for 4 hrs.

## 17. Table S4: LDs targeting multifunctional fluorophores

S. No.	Structure	$\lambda_{\text{ex}}$ (nm)	$\lambda_{\text{em}}$ (nm)	Photostability	Cell Viability & Concentration	PCC (r)	Application	Ref. No.
1.		488	570–620	Yes	>80%, 20 $\mu\text{M}$	0.95	HeLa and Raw 264.7 cells	S1
2.		405	470–560	Yes	$\sim 100\%$ , 30 $\mu\text{M}$	0.80	HeLa cells	S2
3.		405	510–560	Yes	>90%, 100 $\mu\text{M}$ ,	0.857	HeLa, RAW 264.7, L02, HepG2	S3
4.		594	600–700	-	nd	-	A375	S4
5.		405	500–550	Yes	$\sim 90\%$ , 10 $\mu\text{g/mL}$	0.97	Zebrafish, HeLa, HepG2, HL-7702, 4T1, 3T3	S5
6.		405	450–560	Yes	$\sim 85\%$ , 30 $\mu\text{M}$ ,	0.95	HeLa, Zebrafish	S6

7.		488	500–700	Yes	90%, 10 $\mu$ M	0.83–0.96	HeLa, HT22, HepG2, U251	S7
8.		330 – 385	449–520	-	~100%, 100 $\mu$ M, no detectable inhibitory effect	-	HeLa, Liver LO2, Green Alga	S8
9.		488	500–550	Yes	90%, 10 $\mu$ M	0.902	HeLa, Zebrafish	S9
10.		488	~670	Yes	90%, 8 $\mu$ M	-	Hep3B, HepG2, HeLa, IMCD3	S10
11.		488	510–540	Yes	100%, 20 $\mu$ M	0.937	HepG2	S11
12.		488	550-740	Yes	92%, 20 $\mu$ M	0.99	HeLa, HepG2	S12
13.		488	539	Yes	>90%, 50 $\mu$ M	0.50	HeLa,	S13
14.		514	639–740	Yes	>80%, 100 $\mu$ M	-	HCC827 and A549	S14
15.		488	550–650	Yes	~90%, 8 $\mu$ M	0.91,	HeLa, HEK 293T and Cos-7	S15
16.		561	570–700	Yes	>80%, 10 $\mu$ M	-	3T3-L1	S16
17.		370	410-600	Yes	-	0.925	HeLa	S17
18.	  TSIm-1 TSIm-2	404	425-475	Yes	100 $\mu$ M, >70	0.88 (TSIm-2) and 0.82 (TSIm-1)	HeLa, HepG2	Present Work

## 18. Author Contributions

**Mohammad Masood Zafar:** Validation, Formal analysis, Investigation, Data Curation, Writing - Original Draft, **Rashmi Yadav:** Visualization, Validation, Investigation, **Alok Singh:** Methodology, Validation, Investigation, **Nidhi Tyagi:** Conceptualization, Methodology, Validation, Investigation, Resources, Data Curation, Writing - Review & Editing, **Animesh Samanta:** Writing - Review & Editing, Resources, **Rakesh K. Mishra:** Conceptualization, Methodology, Software, Resources, Investigation, Writing - Review & Editing, Visualization, Supervision.

## 19. Supplementary information references:

- S1. C. Li, W. Zhuang, Y. Wang, S. Li, J. Chen, L. Zhou, Y. Liao, M. Chen and J. You, *Dye. Pigment.*, 2022, **204**, 110439.
- S2. W. Bu, X. Guo, X. Lv, Q. Zhang, H. Zuo, Q. Wu, H. Wu, C. Yu, L. Jiao and E. Hao, *Dye. Pigment.*, 2023, **220**, 111735.
- S3. J. Shi, Y. Tian, B. Guo, Y. Wu, J. Jing, R. Zhang and X. Zhang, *Sens. Actuators B: Chem.*, 2019, **284**, 545–552.
- S4. M. S. Filho, P. Dao, A. R. Martin and R. Benhida, *Dye. Pigment.*, 2019, **167**, 68–76.
- S5. F. Yu, X. Jing and W. Lin, *Sens. Actuators B: Chem.*, 2020, **302**, 127207.
- S6. W.-L. Cui, M.-H. Wang, X.-Q. Chen, Z.-H. Zhang, J. Qu and J.-Y. Wang, *Dye. Pigment.*, 2022, **204**, 110433.
- S7. R. Zhou, G. Liu, D. Li, T. Wang, X. Yan, F. Liu, P. Sun, C. Wang and G. Lu, *Sens. Actuators B: Chem.* 2023, **387**, 133772.
- S8. E. Wang, E. Zhao, Y. Hong, J. W. Y. Lam and B. Z. Tang, *J. Mater. Chem. B*, 2014, **2**, 2013–2019.
- S9. M. Peng, J. Yin and W. Lin, *New J. Chem.*, 2018, **42**, 18521–18525.
- S10. X. Zheng, W. Zhu, F. Ni, H. Ai, S. Gong, X. Zhou, J. L. Sessler and C. Yang, *Chem. Sci.*, 2019, **10**, 2342–2348.
- S11. M.-Y. Wu, J.-K. Leung, C. Kam, T. Y. Chou, D. Wang, S. Feng and S. Chen, *Mater. Chem. Front.*, 2021, **5**, 3043–3049.
- S12. X. Shi, S. H. P. Sung, M. M. S. Lee, R. T. K. Kwok, H. H. Y. Sung, H. Liu, J. W. Y. Lam, I. D. Williams, B. Liu and B. Z. Tang, *J. Mater. Chem. B*, 2020, **8**, 1516–1523.
- S13. S. I. Suarez, C. C. Warner, H. B.-Harding, A. M. Thooft, B. VanVeller and J. C. Lukesh, *Org. Biomol. Chem.*, 2020, **18**, 495–499.
- S14. M. Gao, H. Su, S. Li, Y. Lin, X. Ling, A. Qin and B. Z. Tang, *Chem. Commun.*, 2017, **53**, 921–924.
- S15. Y. Yu, H. Xing, H. Park, R. Zhang, C. Peng, H.H.-Y. Sung, I. D. Williams, C. Ma, K. S. Wong, S. Li, Q. Xiong, M.-H. Li, Z. Zhao, B. Z. Tang, *ACS Materials Lett.* 2022, **4**, 159–164.
- S16. C.-J. Wu, X.-Y. Li, T. Zhu, M. Zhao, Z. Song, S. Li, G.-G. Shan, G. Niu, *Anal. Chem.* 2022, **94**, 3881–3887.
- S17. R. S. Fernandes, A. Himaja, B. Ghosh, N. Dey, *ACS Appl. Bio Mater.* 2024, **7**, 8248–8260.
- S18. A. D. Becke, *J. Phys. Chem.*, 1993, **98**, 5648–5652.
- S19. C. Lee, W. Yang and R. G. Parr, *Phys. Rev. B*, 1988, **37**, 785–789.

- S20.** M. J. Frisch, G. W. Trucks, H. B. Schlegel, G. E. Scuseria, M. A. Robb, J. R. Cheeseman, G. Scalmani, V. Barone, G. A. Petersson, H. Nakatsuji, X. Li, M. Caricato, A. V. Marenich, J. Bloino, B. G. Janesko, R. Gomperts, B. Mennucci, H. P. Hratchian, J. V. Ortiz, A. F. Izmaylov, J. L. Sonnenberg, D. Williams-Young, F. Ding, F. Lipparini, F. Egidi, J. Goings, B. Peng, A. Petrone, T. Henderson, D. Ranasinghe, V. G. Zakrzewski, J. Gao, N. Rega, G. Zheng, W. Liang, M. Hada, M. Ehara, K. Toyota, R. Fukuda, J. Hasegawa, M. Ishida, T. Nakajima, Y. Honda, O. Kitao, H. Nakai, T. Vreven, K. Throssell, J. A. Montgomery Jr., J. E. Peralta, F. Ogliaro, M. J. Bearpark, J. J. Heyd, E. N. Brothers, K. N. Kudin, V. N. Staroverov, T. A. Keith, R. Kobayashi, J. Normand, K. Raghavachari, A. P. Rendell, J. C. Burant, S. S. Iyengar, J. Tomasi, M. Cossi, J. M. Millam, M. Klene, C. Adamo, R. Cammi, J. W. Ochterski, R. L. Martin, K. Morokuma, O. Farkas, J. B. Foresman and D. J. Fox, Gaussian 16, Revision C.01, Gaussian, Inc., Wallingford CT, 2016.
- S21.** R. Dennington, T. A. Keith and J. M. Millam, GaussView, Version 6.1, Semichem Inc., Shawnee Mission, KS, 2016.
- S22.** G. Scalmani and M. J. Frisch, *J. Chem. Phys.*, 2010, **132**,114110.